24th INTERNATIONAL CONGRESS ON SOUND AND VIBRATION
23–27 July 2017, London

ISOLATION OF VIBRATIONS INDUCED BY RAILWAY TRAFFIC IN DOUBLE-DECK TUNNELS USING ELASTOMERIC MATS

Arnau Clot
Universitat Politècnica de Catalunya, Laboratori d'Enginyeria Acústica i Mecànica, Terrassa, Spain
email: arnau.clot@upc.edu
Current afiliation: University of Cambridge, Department of Engineering, Cambridge, UK,
email: ac2107@cam.ac.uk

Robert Arcos
Universitat Politècnica de Catalunya, Laboratori d'Enginyeria Acústica i Mecànica, Terrassa, Spain

Behshad Noori
AV Ingenieros, Sant Cugat del Vallès, Terrassa, Spain

Jordi Romeu
Universitat Politècnica de Catalunya, Laboratori d'Enginyeria Acústica i Mecànica, Terrassa, Spain

Modern societies are increasingly concerned with the environmental impact of noise and vibration induced by surface and underground railway traffic in highly populated areas. These induced vibrations may be especially important in the case of double-deck tunnels, where, due to its complexity, new isolation countermeasures may be required. The aim of this paper is to predict, using a three-dimensional semi-analytical model, the isolation efficiency obtained by adding an elastomeric mat at the contact areas between the interior floor and the tunnel structure in double-deck tunnels. The isolation efficiency of the mat is quantified by comparing the soil response during a train pass for different values of the elastomeric mat stiffness. The obtained results show that a suitably defined elastomeric mat can be used as an efficient vibration countermeasure in this type of tunnels.
Keywords: underground vibrations, elastomeric mats, double-deck tunnels.

1. Introduction

The number of underground railways and metro lines constructed world-wide has been continuously growing during the last decades. The requirements and particularities of each railway project have encouraged the development of innovative tunnel designs and construction techniques. One of these designs, recently implemented on Line 9 of the Barcelona underground railway system, is the double-deck tunnel, a tunnel divided into two parts by an intermediate floor which is directly supported by the walls of the tunnel structure. Due to its special geometry, the vibration impact of this structure may not be properly represented by predictive models that consider a simple circular tunnel structure.

The use of analytical and semi-analytical models for the prediction of ground-borne railway-induced vibrations offers clear advantages compared to the alternative empirical or numerical models. In the case of underground railways, one of the most important semi-analytical vibration prediction models is the Pipe-in-Pipe (PiP) model, developed by Forrest and Hunt [1] [2]. The model has been recently extended by Hussein et al. to the case where the tunnel is embedded into a layered half-spaces [3]. Hussein and Hunt also proposed a method, based on the computation of the radiated vibration power flow, for evaluating the variations of underground railway-induced vibrations under track design modifications [4]. An alternative type of evaluation has been presented by Lopes et al. [5], [6], who developed a numerical model of the tunnel-soil-building system and used it for studying the effect that different soil stratifications or a change in the under slab mat stiffness had on the building response to railway traffic. The first semi-analytical double-deck model presented in the literature, which coupled the PiP model to an infinite strip plate, was proposed by Clot et al. [7]. The model has been used by Clot et al. [8, 9] to compare the power and energy flows radiated by a double-deck tunnel structure with that radiated by a simple tunnel for different types of harmonic excitations.

In this paper, the vibration induced by a train circulating in a double-deck tunnel structure is studied. The main contributions of this work is the addition of a vehicle and track models to the double-deck tunnel model presented in [7]. The complete vehicle-track model is then used to study the isolation efficiency of a new potential vibration countermeasure: the addition of an elastomeric mat between the interior floor and the tunnel structures. The remainder of the paper is structured as follows: The proposed prediction model is briefly described in Section 2, the results obtained are presented in Section 3, and the main conclusions of the work are detailed in Section 4.

2. Model description

This section describes the proposed semi-analytical vehicle-track-tunnel-soil model that is used for predicting the isolation efficiency of the elastomeric mat as a new vibration countermeasure for double-deck tunnels. The section is divided into two subsections: the considered double-deck tunnel model is summarised in the first one and the vehicle-track coupling is briefly described in the second.

2.1 Double-deck tunnel model

The semi-analytical model used for computing the response of a double-deck tunnel structure is represented in Figure 1. The main hypothesis of the model are summarised here, but additional details can be found in [7].

- The strains are small enough to assume linear elasticity and the track-tunnel-soil structure is geometrically and mechanically invariant in the train circulation direction.
- The rails are modelled as infinite Bernoulli-Euler beams of constant cross-section coupled to the tunnel interior floor with direct fixation fasteners. The rails are separated at a distance d_r and equidistant from the tunnel walls.
- The rail pads are modelled as a continuous mass-less distribution of springs, with a constant stiffness per metre k_F, and dashpots, with a constant viscous damping per metre c_F.
- The interior floor is modelled as an infinite thin strip plate with a constant rectangular cross-section.
- An elastomeric mat is implemented between the interior floor and the tunnel. The mat is modelled as a continuous mass-less distribution of springs, with a constant stiffness per metre k_M, and dashpots, with a constant viscous damping per metre c_M.
- The tunnel is modelled as an infinite thin cylindrical shell, as it is considered in [1].
- The soil is modelled as a viscoelastic full-space, as it is considered in [1].

In the wavenumber-frequency domain ($k-\omega$ domain), the response $U(k,\omega)$ of the double-deck tunnel system to an external force $F(k,\omega)$ is given by $U(k,\omega) = H(k,\omega)F(k,\omega)$, where $H(k,\omega)$ is the frequency response function (FRF) of the system. The computation of $H(k,\omega)$ requires to know the coupling forces that exist between the rail, floor and tunnel subsystems. With the considered coupling conditions, the (symmetric) rail-floor F_{rf} and floor-tunnel F_{ft} interaction forces caused by

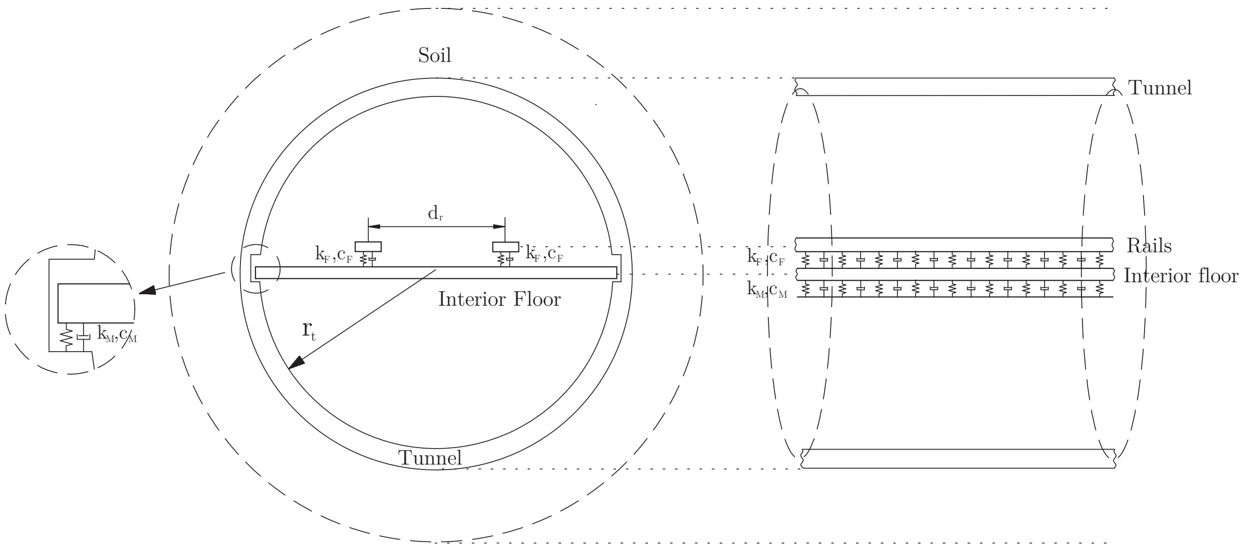

Figure 1: Considered model for a double-deck tunnel structure with a track.

an external force $F(k,\omega) = 1$ can be obtained solving

$$\begin{bmatrix} \frac{1}{s_F} + H^r + H^p_{11} + H^p_{12} & H^p_{13} + H^p_{14} \\ H^p_{31} + H^p_{32} & \frac{1}{s_M} + H^p_{33} + H^p_{34} + H^t_{33} - H^t_{34} \end{bmatrix} \begin{Bmatrix} F_{rf} \\ F_{ft} \end{Bmatrix} = \begin{Bmatrix} H^r \\ 0 \end{Bmatrix}, \tag{1}$$

where H^r is the FRF of an infinite beam, H^p_{ij} is the FRF of a thin strip plate, H^t_{ij} is the FRF of the PiP model, and where the parameters $s_F = k_F + \mathrm{i}\omega c_F$ and $s_M = k_M + \mathrm{i}\omega c_M$ includes the fasteners elastomeric mat effects, respectively. In the notation used, the positions where the rails are connected to the interior floor are identified as 1 and 2, and the positions where the interior floor is connected to the tunnel are identified as 3 and 4.

2.2 Vehicle-track coupling

The train is assumed to move along the tunnel at a constant speed v_t, and to be composed of several equal cars. The vehicle-track coupling considers that the train wheels are always in contact with the rails, and that the horizontal interaction is much less significant than the vertical interaction. The dynamic component of the contact force is considered to be exclusively caused by the rail unevenness, which is assumed to be equal in both rails. The wheel-rail contact is represented using a linearised Hertz contact model.

Following the formulation presented in [10], for each value of the moving frequency $\tilde{\omega}$ (frequency emitted by the moving source) the vector of dynamic wheel-rail contact forces $\boldsymbol{f}^{w/r}$ can be obtained from

$$\boldsymbol{f}^{w/r}(\tilde{\omega}) = [\boldsymbol{C}_{\text{vehicle}} + \boldsymbol{C}_{\text{track}}]\,\boldsymbol{U}_{\text{rough}}(\tilde{\omega}) \tag{2}$$

where $\boldsymbol{C}_{\text{vehicle}}$ is the vehicle compliance matrix, $\boldsymbol{C}_{\text{track}}$ is the track compliance matrix, and $\boldsymbol{U}^{\text{rough}}$ is the vector of rail roughness profiles at all the contact points.

The elements of $\boldsymbol{C}_{\text{vehicle}}$ are obtained from the considered rolling-stock dynamical model. The rolling-stock is represented as mass-spring-damper system in which it is assumed that the interaction between the different wheels of a car and the interaction between the different cars can be neglected. The system consists of a rigid body with a mass m'_w, representing the combined wheel and "1/2-axle" mass, connected to a mass m'_c, which represents the combined "1/4-bogie" and "1/8-car" mass, by a spring-dashpot system $k_{ps} - c_{ps}$, representing the car primary suspension. The linearised Hertz contact is added by considering a spring of stiffness k_{Hz} at the wheel-rail contact point. With these assumptions, the vehicle compliance matrix can be simply expressed as a unitary matrix multiplied by a scalar quantity.

The elements of $\boldsymbol{C}_{\text{track}}$ can be obtained from the response of the system to the set of dynamic wheel forces. In a moving frame of reference $\hat{x} = x - v_t t$, this response can be expressed as [10]

$$u(\hat{x},t) = \frac{1}{2\pi}\int_{-\infty}^{\infty}\sum_{n=1}^{N_c}\left[\frac{1}{2\pi}\int_{-\infty}^{\infty} H(k,\tilde{\omega}+kv_t)\mathrm{e}^{\mathrm{i}k(\hat{x}-x_{n,0})}\mathrm{d}k\right] f_n^{w/r}(\tilde{\omega})\mathrm{e}^{\mathrm{i}\tilde{\omega}t}\mathrm{d}\tilde{\omega}, \tag{3}$$

where N_c is the number of contact points and $x_{n,0}$ is the position of the n-th contact at t = 0 s. The element $C_{\text{track},ln}$ can be obtained substituting $\hat{x} = x_l$ in the bracketed expression of Eq. (3). Note that in this case $H(k,\tilde{\omega}+kv_t)$ refers to the rail response in the double-deck tunnel model previously described, instead of to the soil response.

The velocity at any position can be obtained by derivation. The resulting expression is

$$v(\hat{x},t) = \frac{1}{2\pi}\int_{-\infty}^{\infty}\sum_{n=1}^{N_c}\left[\frac{1}{2\pi}\int_{-\infty}^{\infty} \mathrm{i}(\tilde{\omega}+kv_t)H(k,\tilde{\omega}+kv_t)\mathrm{e}^{\mathrm{i}k(\hat{x}-x_{n,0})}\mathrm{d}k\right] f_n^{w/r}(\tilde{\omega})\mathrm{e}^{\mathrm{i}\tilde{\omega}t}\mathrm{d}\tilde{\omega}. \tag{4}$$

The results of computing Eq. (4) for different values of the elastomeric mat stiffness are presented in the next section.

3. Results

This section presents some results that have been obtained with the vehicle-track model for a double-deck tunnel previously described. The section has been divided into three subsections: First, the considered mechanical properties for the different subsystems are described, then, the response of the rails-floor subsystem to a train pass is considered and, finally, the responses of the soil to a train pass for different values of the elastomeric mat stiffness are compared.

3.1 Mechanical and geometrical parameters considered

The geometrical and mechanical parameters considered in the calculations are detailed here. The considered vehicle consist of three equal cars and its mechanical parameters, which do not represent any particular type of train, can be found in Table 1. Also, the distance between the wheels of a bogie is 2.2 m, the distance between the bogies of a car is 15 m, and the distance between the same bogie of two consecutive cars is 22 m. The rail and interior floor parameters are described in Table 2 and the tunnel and soil parameters in Table 3. For clarity, symbols are only used for those parameters that have been defined in the previous section.

In general, the cross-section of the tunnel interior floor can differ considerably from the rectangular one that has been assumed. In order to take this fact into account, an equivalent thin plate has been determined by comparing the transverse response predicted by the considered analytical model with the one obtained with a two-dimensional Finite Element (FE) model of the plate structure. In this work, the cross-section of the interior floor implemented in some stretches of Line 9 of Barcelona Metro Network has been considered (see Figure 2a).

The equivalent plate has been obtained with a two-steps procedure. First, the equivalent thickness of the floor has been obtained by minimising the difference between the transversal eigenmodes of both models. Then, the equivalent Young modulus has been obtained by minimising the difference

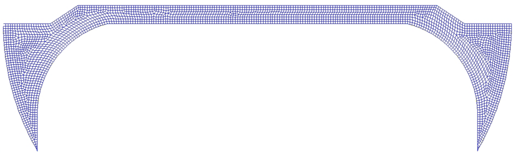

(a) FE model of the interior floor considered in this work.

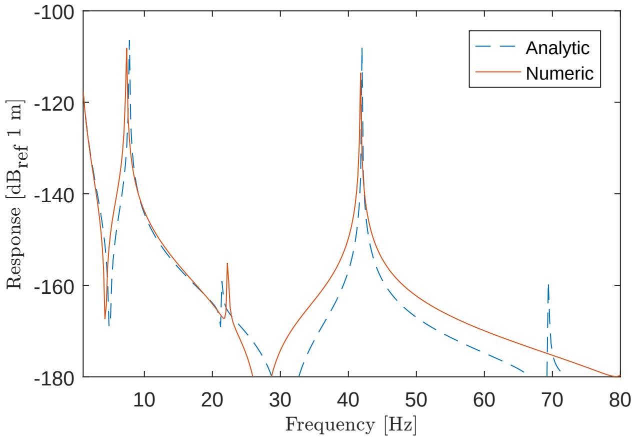

(b) Transverse response of the numeric model and of the equivalent analytic model.

Table 1: Mechanical parameters used for the vehicle and for the fasteners.

Parameter	Value	Parameter	Value
m'_c	5000 kg	k_F	$20 \cdot 10^6$ N/m^2
m'_w	1000 kg	c_F	$6.3 \cdot 10^3$ N·s/m^2
k_{ps}	10^6 N/m	c_{ps}	$3.5 \cdot 10^4$ N·s/m
k_{Hz}	10^9 N/m	v_t	20 m/s

Table 2: Mechanical parameters used for the rail and interior floor models (* *Equivalent model values*).

Rail Parameter	Value	Floor Parameter	Value
Cross-sectional area	$6.93 \cdot 10^{-3}$ m^2	Width	10.9 m
Second moment of area	$23.5 \cdot 10^{-6}$ m^4	Thickness*	0.7 m
Young modulus	$207 \cdot 10^9$ N/m^2	Young modulus*	$3.95 \cdot 10^9$ N/m^2
Density	7850 kg/m^3	Poisson ratio	0.175
d_r	1.5 m	Density	3000 kg/m^3

Table 3: Mechanical parameters used for the tunnel and soil models.

Tunnel Parameter	Value	Soil Parameter	Value
Radius	5.65 m	Density	2000 kg/m^3
Thickness	0.4 m	Poission ratio	0.44
Young modulus	$50 \cdot 10^9$ N/m^2	Young modulus	$550 \cdot 10^6$ N/m^2
Poisson ratio	0.175	P-wave damping	0.03
Density	3000 kg/m^3	S-wave damping	0.03

between the response of both models to a point load. The result of this last step is represented in Figure 2b and the parameters obtained are the ones presented in Table 2. The authors are currently working on extending this methodology to a three-dimensional study instead of a 2D one.

3.2 Thin plate response

The response of the interior floor structure to a train pass is initially studied by imposing $H_{ij}^t = 0$ in Eq. (1), which represents the case where the tunnel-soil structure is assumed to be infinitely rigid. Following a common approach in the prediction of railway vibrations [6, 10], the rail roughness has been modelled as a stochastic random process characterized by an empirical power spectral density function. The profile sampling has been performed ensuring that its length is large enough for computing the whole train pass and that its step increment Δx is small enough to obtain the soil response in all the range of frequencies of interest. A small sample of a generated roughness profile can be seen in Figure 3 (a).

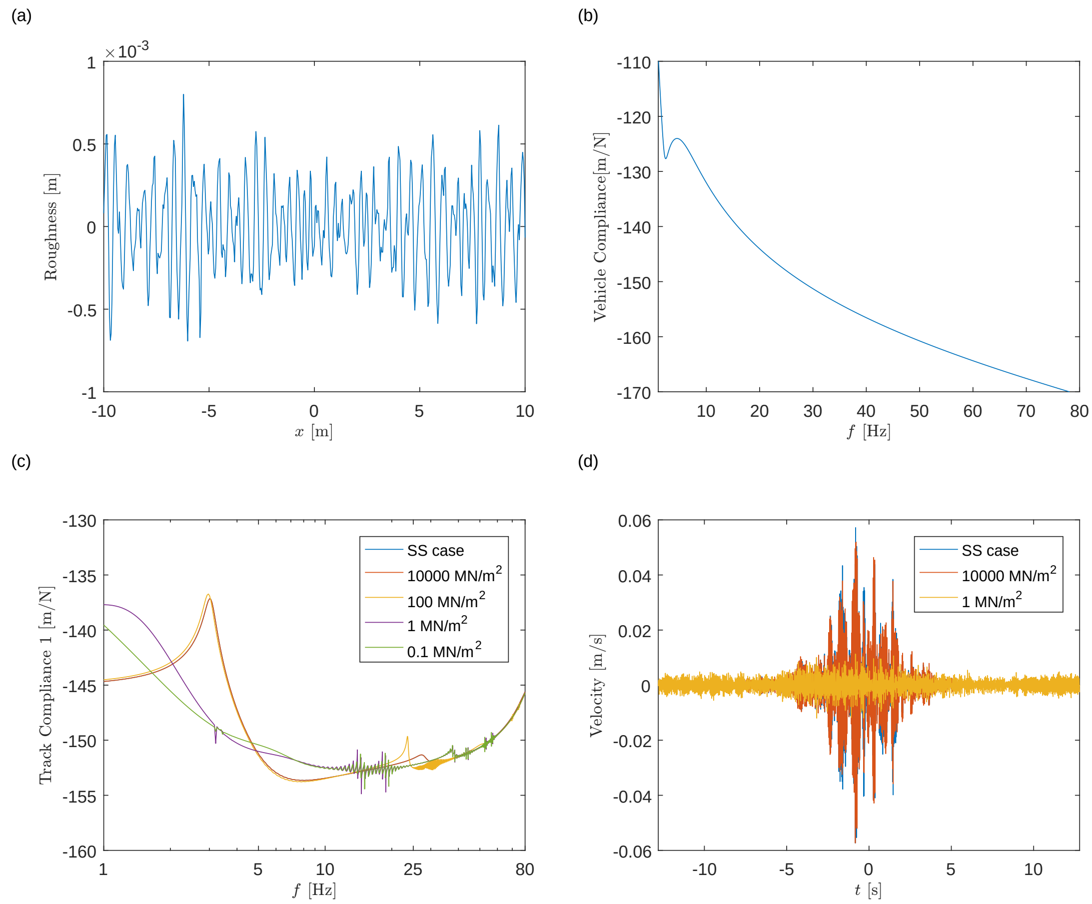

Figure 3: Results obtained for the case of a thin plate formulation. (a) An example of the random roughness profile considered. (b) Vehicle compliance. (c) Track compliance at the first wheel position for different values of the mat stiffness. (d) Velocity of a point of the plate for different values of the mat stiffness.

Figures 3 (b) and (c) show one of the diagonal elements of the vehicle compliance matrix $\boldsymbol{C}_{\text{vehicle}}$ and the first element of the track compliance matrix $\boldsymbol{C}_{\text{track}}$, respectively. The track compliance has been computed for different values of the elastomeric mat stiffness $k_M = 10^5$, 10^6, 10^8 and 10^{10} N/m^2. In all cases, a viscous damping $c_M = 10^5$ N·s/m^2 has been used. The case where the strip plate is simply supported (defined as SS case in the legend) instead of free has been also represented in the figure.

The results show that the track compliance is clearly affected by a modification of the mat stiffness, giving some insights of its potential efficiency as vibration countermeasure. The results also show that there is practically no difference between the case where $k_M = 10^{10}$ N/m^2 and the simply supported case. This result, despite being expected, is an interesting partial check of the correctness of the considered formulation. Some small instabilities can be also observed at certain frequencies of the compliance curves, the origin and the importance of this instabilities is currently being studied by the authors.

In Figure 3 (d), the velocity at a position of the interior floor is presented for the simply supported case, and for $k_M = 10^6$ N/m^2 and 10^{10} N/m^2. The results have been computed using Eq. (4) and show that the amplitude of the vibration velocity is significantly reduced for the case of the softer mat. A more detailed study of its effect, however, requires to consider the whole vehicle-track-tunnel-soil system.

3.3 Soil response to a train pass

Figure 4 shows the time history and the frequency spectrum of the radial velocity of the soil for three different values of the mat stiffness: $k_M = 3 \cdot 10^5$ N/m^2, $3 \cdot 10^6$ N/m^2 and $3 \cdot 10^7$ N/m^2. The considered position is situated at a radial distance $r = 12$ m from the tunnel centre and at an angular position $\theta = \pi/3$ rad, measured clockwise from a horizontal axis that contains the tunnel interior floor.

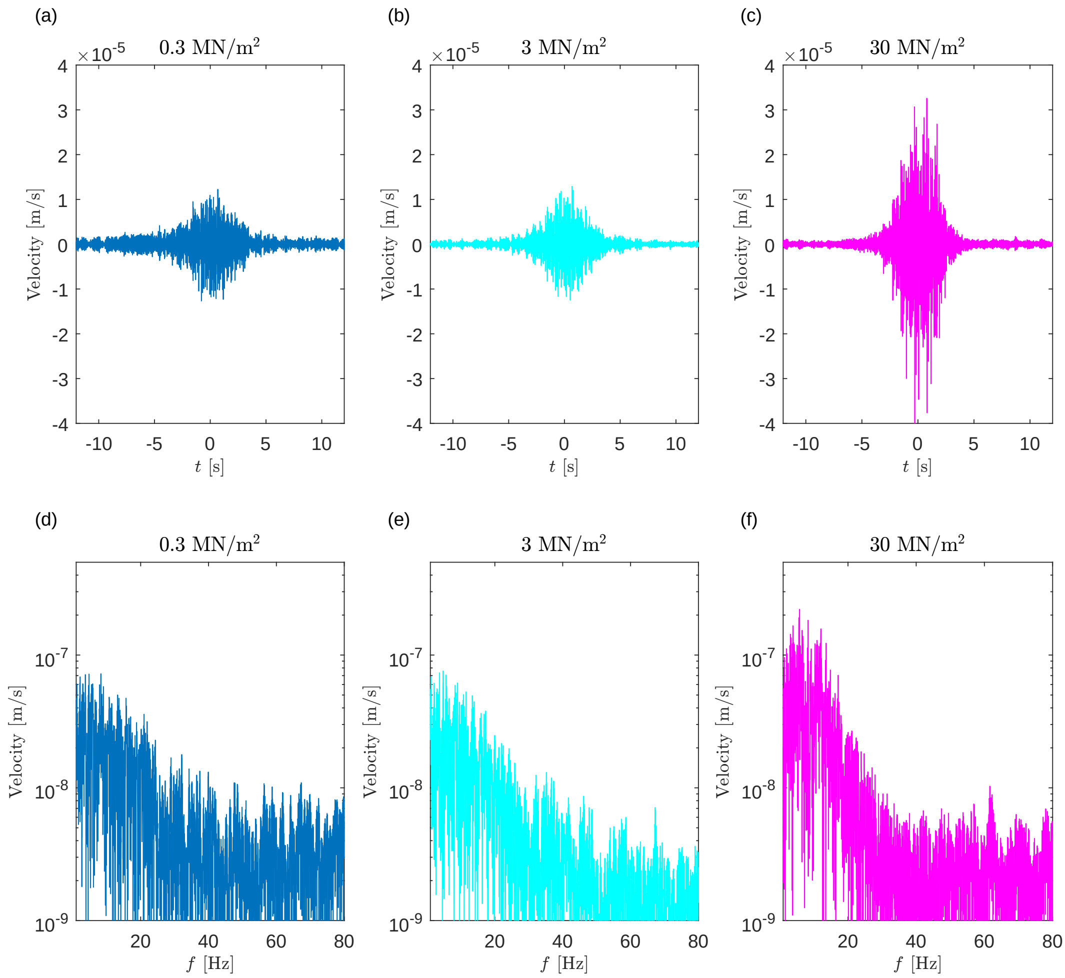

Figure 4: Radial velocity at a position of the soil for different values of the elastomeric mat stiffness. (a)-(c) Time history. (d)-(e) Frequency content.

The results show a considerable reduction of the soil velocity in the case where a soft elastomeric mat is implemented. Also, the content of the three response spectra is particularly high at low frequencies. The sensibility of the response to the modification of other parameters of the model, such as the damping values c_M or the vehicle parameters, is currently being studied.

4. Conclusions

This work presents an initial evaluation of the isolation efficiency of an innovative vibration countermeasure potentially applicable in double-deck tunnel structures: the addition of an elastomeric mat at the contact between the interior floor and the tunnel. The predictions have been performed coupling a vehicle model to a previously developed semi-analytical model for a double-deck tunnel-soil system. A procedure that allows to include different types of interior floor cross-section geometries in the model has been also described.

It has been found that the modification of the elastomeric mat stiffness can result into significant variations of the system response. In particular, for the set of geometrical and mechanical parameters considered, the results predict a significant reduction of the soil velocity when the implemented elastomeric mat is a relatively soft.

The results presented in this work show the potential efficiency of this innovative vibration countermeasure. However, these results only describe the response at a certain position of the soil instead of a global effect. The authors are currently working on the development of an efficient and accurate method for computation the total energy flow radiated by the structure during a train pass.

REFERENCES

1. Forrest, J. A. and Hunt, H. E. M. A three-dimensional tunnel model for calculation of train-induced ground vibration, *J Sound Vib*, **294** (4-5), 678–705, (2006).

2. Forrest, J. A. and Hunt, H. E. M. Ground vibration generated by trains in underground tunnels, *J Sound Vib*, **294** (4-5), 706–736, (2006).

3. Hussein, M., François, S., Schevenels, M., Hunt, H., Talbot, J. and Degrande, G. The fictitious force method for efficient calculation of vibration from a tunnel embedded in a multi-layered half-space, *Journal of Sound and Vibration*, **333** (25), 6996–7018, (2014).

4. Hussein, M. F. M. and Hunt, H. E. M. A power flow method for evaluating vibration from underground railways, *Journal of Sound and Vibration*, **293**, 667–679, (2006).

5. Lopes, P., Alves Costa, P., Calçada, R. and Silva Cardoso, A. Influence of soil stiffness on building vibrations due to railway traffic in tunnels: Numerical study, *Computers and Geotechnics*, **61**, 277–291, (2014).

6. Lopes, P., Costa, P. A., Ferraz, M., Calçada, R. and Cardoso, A. S. Numerical modeling of vibrations induced by railway traffic in tunnels: From the source to the nearby buildings, *Soil Dynamics and Earthquake Engineering*, **61-62**, 269–285, (2014).

7. Clot, A., Arcos, R., Romeu, J. and Pàmies, T. Dynamic response of a double-deck circular tunnel embedded in a full-space, *Tunnelling and Underground Space Technology*, **59**, 146–156, (2016).

8. Clot, A., Romeu, J., Arcos, R. and Martín, S. R. A power flow analysis of a double-deck circular tunnel embedded in a full-space, *Soil Dynamics and Earthquake Engineering*, **57**, 1–9, (2014).

9. Clot, A., Romeu, J. and Arcos, R. An energy flow study of a double-deck tunnel under quasi-static and harmonic excitations, *Soil Dynamics and Earthquake Engineering*, **89**, 1–4, (2016).

10. Lombaert, G. and Degrande, G. Ground-borne vibration due to static and dynamic axle loads of InterCity and high-speed trains, *Journal of Sound and Vibration*, **319** (3-5), 1036–1066, (2009).